Microfluidic shrinking of microbubble contrast agents

Vaskar Gnyawali
Mechanical and Industrial Engineering, Ryerson University
Institute for Biomedical Engineering, Science and Technology
Keenan Research Center, St. Michaels Hospital
Toronto, Canada
vgnyawali@ryerson.ca

Byeong-Ui Moon
Mechanical and Industrial Engineering, Ryerson University
Institute for Biomedical Engineering, Science and Technology
Keenan Research Center, St. Michaels Hospital
Toronto, Canada
b.u.moon14@gmail.com

Jennifer Kieda
Electrical and Computer Engineering, Ryerson University
Institute for Biomedical Engineering, Science and Technology
Keenan Research Center, St. Michaels Hospital
Toronto, Canada
jennifer.kieda@ryerson.ca

Raffi Karshafian
Department of Physics, Ryerson University
Institute for Biomedical Engineering, Science and Technology
Keenan Research Center, St. Michaels Hospital
Toronto, Canada
karshafian@ryerson.ca

Michael C. Kolios
Department of Physics, Ryerson University
Institute for Biomedical Engineering, Science and Technology
Keenan Research Center, St. Michaels Hospital
Toronto, Canada
mkolios@ryerson.ca

Scott S. H. Tsai
Mechanical and Industrial Engineering, Ryerson University
Institute for Biomedical Engineering, Science and Technology
Keenan Research Center, St. Michaels Hospital
Toronto, Canada
scott.tsai@ryerson.ca

***Abstract*—We develop a new microfluidic technique to generate lipid-stabilized microbubbles of 1-7 μm diameter. We shrink microbubbles that are initially O(100) μm in diameter by using a vacuum system. We use a polydimethylsiloxane (PDMS) microfluidic device to generate microbubbles in a conventional flow focusing orifice. The bubbles pass through a serpentine channel while under vacuum pressure, and shrink to O(1) μm in diameter. We control a single parameter, the vacuum pressure, in the vacuum channels that are fabricated adjacent to the serpentine channel. We demonstrate that the shrunk microbubbles are stable for at least 75 minutes in atmospheric conditions. We anticipate that this simple approach can be used to generate microbubbles for ultrasound (US) imaging and therapeutic applications by increasing the throughput of the microfluidic microbubble generating system.**

***Index Terms*—Microfluidics, Microbubble, Ultrasound, Contrast agent**

I. Introduction

Lipid-stabilized gas microbubbles are widely used for ultrasound (US) diagnostics and therapeutic applications [1]. These microbubbles have a typical diameter of 1-7 μm, and can be intravenously injected into the circulation of the body. When used for US imaging applications, the microbubbles help emit strong US echo signals, which enhance the image contrast between the blood vessels and surrounding tissues [2]. For therapeutic applications, US exposed microbubbles increase the reversible permeability of the cell membrane to facilitate the selective gene and/or drug delivery to target cells for cancer, cardiovascular, and blood-brain-barrier treatments [3] [4] [5] [6]. The microbubble size has an important effect on the microbubble US frequency response. To ensure uniformity of microbubble response, monodispersed microbubbles are desired.

Conventional microbubble production techniques include sonication [7], high shear emulsification [8], inkjet printing [9] and coaxial eletrohydrodynamic atomization (CEHDA) [10]. Microbubbles generated by these techniques are typically polydisperse and conventional production techniques do not have effective control on microbubble sizes. DEFINITY® is a commercially available and US Food and Drug Administration (FDA) approved microbubble solution. DEFINITY® microbubbles average 1-3 μm in diameter and are also highly polydispersed, with maximum size reaching 20 μm in diameter [12]. As a result when using DEFINITY®, a post processing filtration technique is required to obtain the microbubbles of desired sizes.

A recently developed microfluidic technique generates monodispersed microbubbles with precise control on microbubble size [11] [12]. Although the size of the generated microbubbles in microfluidics depends on the continuous phase fluid flow rate and inlet gas pressure, the limiting factor for producing smaller microbubbles is the size of the flow focusing orifice [12]. Orifices of less than 10 μm in

978-1-5386-3383-0/17/$31.00 ©2017 IEEE

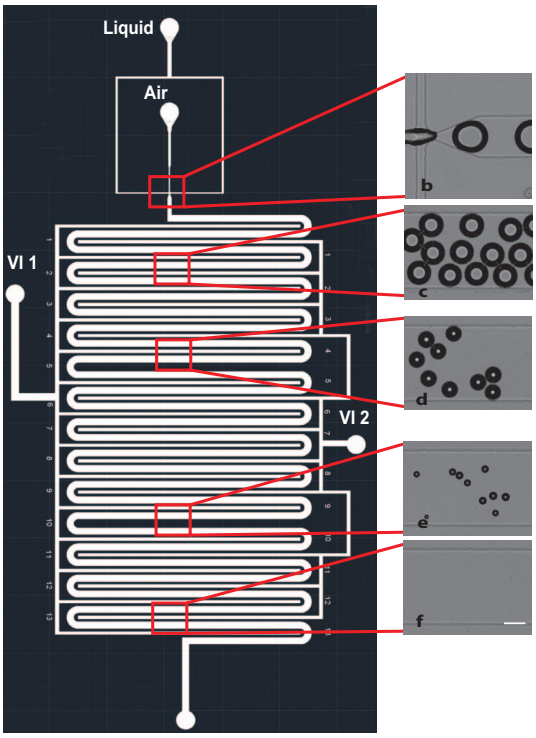

Fig. 1. (a) Design of our microfluidic device. Experimental images of the microbubbles (b) generated at the orifice and (c-f) shrunken in the channel, at the vacuum pressure P_v = -50 kPa, as they flow downstream towards the outlet. We supply a negative vacuum pressure to the vacuum channels using vacuum inlets VI1 and VI2. The scale bar represents 50 μm.

width are required to generate microbubbles of desired 1-7 μm diameter range [12] [13]. Mold fabrication for such microfluidic geometries requires complex and expensive microfabrication protocols [14]. Another issue with smaller flow focusing orifices is that they can be easily clogged due to solution impurities and PDMS debris accumulation at the orifice junction [14] [15].

In this article, we show a simple and effective technique to generate microbubbles using a conventional flow focusing orifice (20 μm) and shrink them to desired sizes in a microfluidic device for US imaging and therapeutic applications. Our microfluidic design consists of two adjacent set of channels, one for microbubble flow and one for applying the vacuum. This enables microbubble shrinkage from $O(100)$ μm to $O(1)$ μm in diameter. The shrinkage is controlled by tuning only one single parameter, the vacuum pressure, in the vacuum channels. Importantly, our method reduces the problems of orifice clogging and mold manufacturing complexities.

II. Material and Methods

We use air as the dispersed phase and a mixture of lipids, glycerol (Sigma Aldrich Corporation, St. Louis, MO, USA), and pluronic F-68 (Fisher Scientific, Pittsburgh, PA, USA) in a 1:1:1 volumetric ratio as the continuous liquid phase. The lipid mixture is prepared using 9:1 molar ratio of 1,2-distearoyl-sn-glycero-3-phosphocoline (DSPC) (Avanti Polar Lipids, Alabaster, AL, USA) and 1,2-distearoyl-sn-glycero-3-phosphoethanolamine-N [methoxy-(polyethylene glycol)-5000] (DSPE-PEG5000) (Avanti Polar Lipids, Alabaster, AL, USA) in saline solution (lipid concentration of 1.5 mg/mL). Our lipid solution composition is similar to the commercially available DEFINITY® microbubbles [16].

We use photolithography to fabricate the designs on a wafer and then soft lithography to make the microfluidic channels. Briefly, we spin-coat a 80 μm thick film of SU-8 2075 on a silicon wafer. Computer-aided design (CAD) software (AutoCAD 2010, Autodesk, Inc., Dan Rafael, CA, USA) is used to design the microfluidic geometries, which are then patterned on a silicon wafer using a negative photoresist. The pattern formed on the wafer by photolithography is used as a mold to transfer the features to a polydimethylsiloxane (PDMS, Sylgard 184 silicone elastomer kit, Dow Corning, Midland, MI, USA) slab using conventional soft lithography techniques [17]. A 1 mm diameter biopsy punch (Integra Miltex, Inc., Rietheim-Weilheim, Germany) is then used to punch inlets/outlets. The final processing step is to bond the PDMS slab, with the pattern, irreversibly on to a glass microscope slide using oxygen plasma (Harrick Plasma, Ithaca, NY, USA).

Our microfluidic device has two inlets for continuous and disperse phases, two vacuum inlets, and an outlet (Fig. 1a). The flow focusing orifice is 20 μm wide (shown in Fig. 1b), which is connected to a serpentine channel that is 350 μm wide and 350 mm long. The 150 μm wide vacuum lines on both sides of the serpentine channel keeping 175 μm distance with the serpentine channel (Fig. 1a). All the microchannels have a height of h = 80 μm.

In our experiments, the continuous phase, lipid solution, is supplied using a syringe pump (Harvard Instruments, Holliston, MA, USA) at a constant flow rate of Q = 4 μLmin^{-1} while the disperse phase, pressurized air, is supplied at P_a = 4 psi. We vary the vacuum pressure in the range of P_v = 0 to -90 kPa using a Mityvac hand vacuum pump (Mityvac, St. Louis, MO, USA) integrated with a pressure gauge.

We capture images and videos of the channels using a high speed camera (Phantom M110, Vision Research, Wayne, NJ, USA) attached to an inverted microscope (Olympus Corp., Tokyo, Japan). The videos are recorded at 100 fps with an exposure time of 500 μs. We use ImageJ software to measure the bubble initial diameter, D_i, right after exit from the orifice. The smallest bubble diameter along the serpentine channel detectable by 10x objective in a microscope is considered as the final bubble diameter, D_f.

III. Result and Discussion

A. Microbubble shrinkage

The images of microbubbles shrinking in the device when applied vacuum pressure of P_a = -50 kPa is applied are shown in Fig. 1b-f. The microbubbles are generated at the orifice (Fig. 1b) and flow downstream in the serpentine channel. These microbubbles gradually shrink (Fig. 1c-f) while flowing downstream because of the low pressure vacuum lines interdigitated beside the serpentine channel.

978-1-5386-3383-0/17/$31.00 ©2017 IEEE

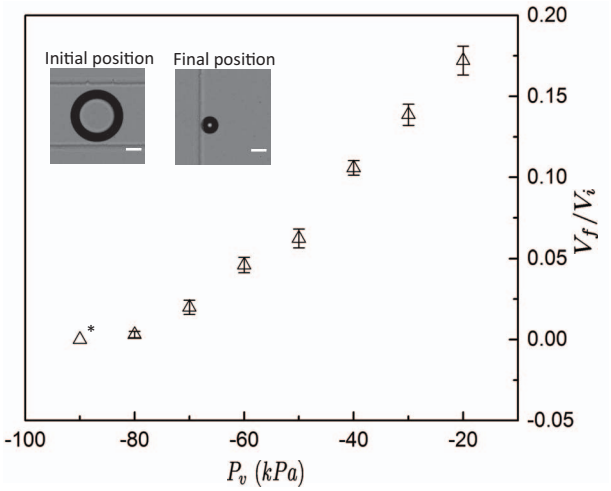

Fig. 2. Normalized microbubble volume, V_f/V_i, as a function of the applied vacuum pressure, P_v. Insets show representative experimental images of the microbubbles at the initial and final measuring positions for an experiment with P_v = -50 kPa. The error bars represent one standard deviation of 10 different microbubble measurements. The scale bar represents 50 μm.

As the initial diameter, D_i, of the microbubbles is larger than the channel height, h = 80 μm, they are squeezed when flowing through the channel. However, near the outlet, the shrunken microbubbles are smaller than the height of the channel and hence they are spherical. To compare the equivalent effect at the orifice and the outlet, we compare initial volume, V_i, and final volume, V_f, to characterize the shrinkage. We calculate the initial volume, V_i, using diameter of the discoid microbubbles and the height of the microchannel next to the orifice. The equations to calculate the initial volume is explained elsewhere [18].

The comparison between the normalized final microbubble volume, V_f/V_i, and the applied vacuum pressure, P_v, is shown in Fig. 2. Experiments show that the microbubbles naturally shrink by 45 %, within the length of the microchannel, without applying vacuum pressure, P_v = 0. Similar natural shrinkage observations have been reported in the literature [21], [22]. This shrinkage effect is due to the pressure-driven nature of the flow in the microfluidic device and is governed by the Henry's law. According to Henry's law, the concentration of dissolved air in the liquid is higher at higher pressure [19]. To maintain the thermodynamic equilibrium in the continuous phase liquid, the air inside the microbubbles diffuses to the continuous phase liquid, as the result, the microbubbles shrink. However, this natural shrinking is a slow process [19]. To speed up the shrinking process we apply a vacuum pressure. The vacuum shrinkage provides an additional advantage of precise control on the size of the resulting microbubbles. In our device, we exploit the gaseous semi-permeability of PDMS [20] to permeate the dissolved gas in the continuous liquid to the adjacent vacuum microchannels from the main microchannel. To conserve the equilibrium, microbubbles shrink. Fig. 2 shows the variation of microbubbles shrinkage versus the vacuum pressure, P_v. This figure shows that the the ratio of the initial to final bubble volume V_f/V_i is close to 0 at the applied vacuum pressure P_v = - 90 kPa (indicated by '*' in the Fig. 2).

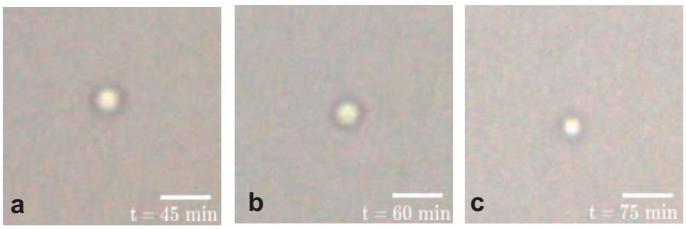

Fig. 3. Experimental sequential images of a single shrunken microbubble taken at (a) t = 45 min, (b) t = 60 min, and (c) t = 75 min after exit from at the outlet of the microfluidic device. The scale bar represents 5 μm.

B. Stability of the shrunken microbubbles

The microbubble shrinking is not due to the higher pressure compression in the microfluidic channel. During the shrinking process, the applied vacuum removes the dissolved gas from the continuous phase liquid. As a response, the air molecules inside the microbubbles diffuse into the continuous phase liquid to maintain thermodynamic equilibrium. Therefore, these shrunken microbubbles do not revert back to their original size after exposed to atmospheric pressure and hence, they remain stable. Fig. 3 shows sequencial images of a shrunken microbubble, approximately 2 μm in diameter, which maintain a stable size for at least 75 minutes after exiting the microfluidic device. The images were taken t = 45 min (Fig. 3a), t = 60 min (Fig. 3b), and t = 75 min (Fig. 3c) after the microbubble was collected from the outlet of the microfluidic device. For this experiment, we used vacuum pressure P_v = -90 kPa and the images were observed using a 40x objective.

IV. Conclusion

We developed a novel technique to generate and shrink the microbubbles to a desired size for US applications using vacuum pressure and microfluidics. These shrunken microbubbles are stable for at least 75 minutes after they are removed from the microfluidic device.

Acknowledgment

The authors would like to acknowledge funding support from the Natural Sciences and Engineering Research Council (NSERC) Discovery grants program and an NSERC Engage grant (grant no. EGP 491921-15) held in collaboration with the industrial partner, MD Precision Inc.

References

[1] M. J. K. Blomley, J. C. Cooke, E. C. Unger, M. J. Monaghan, and D. O. Cosgrove, "Science, medicine, and the future: Microbubble contrast agents: a new era in ultrasound, Bmj, vol. 322, no. 7296, pp. 12221225, 2001.

[2] P. a Dayton, K. E. Morgan, a L. Klibanov, G. H. Brandenburger, and K. W. Ferrara, "Optical and acoustical observations of the effects of ultrasound on contrast agents., IEEE Trans. Ultrason. Ferroelectr. Freq. Control, vol. 46, no. 1, pp. 220232, 1999.

978-1-5386-3383-0/17/$31.00 ©2017 IEEE

[3] R. Karshafian, S. Samac, P. D. Bevan, and P. N. Burns, "Microbubble mediated ssonoporation of cells in suspension: Clonogenic viability and influence of molecular size on uptake, Ultrasonics, vol. 50, no. 7, pp. 691697, 2010.
[4] E. Stride and M. Edirisinghe, "Special issue on microbubbles: From contrast enhancement to cancer therapy, Med. Biol. Eng. Comput., vol. 47, no. 8, pp. 809811, 2009.
[5] K. Hynynen, "Ultrasound for drug and gene delivery to the brain, Adv. Drug Deliv. Rev., vol. 60, no. 10, pp. 12091217, 2008.
[6] R. Bekeredjian, P. A. Grayburn, and R. V. Shohet, "Use of ultrasound contrast agents for gene or drug delivery in cardiovascular medicine, J. Am. Coll. Cardiol., vol. 45, no. 3, pp. 329335, 2005.
[7] E. Stride and M. Edirisinghe, "Novel microbubble preparation technologies, Soft Matter, vol. 4, pp. 23502359, 2008.
[8] K. Bjerknes, K. Dyrstad, G. Smistad, and I. Agerkvist, "Preparation of polymeric microcapsules: formulation studies, Drug Dev. Ind. Pharm., vol. 26, no. 8, pp. 84756, 2000.
[9] M. Kukizaki and M. Goto, "Spontaneous formation behavior of uniform-sized microbubbles from Shirasu porous glass (SPG) membranes in the absence of water-phase flow, Colloids Surfaces A Physicochem. Eng. Asp., vol. 296, no. 13, pp. 174181, 2007.
[10] U. Farook, H. B. Zhang, M. J. Edirisinghe, E. Stride, and N. Saffari, "Preparation of microbubble suspensions by co-axial electrohydrodynamic atomization, Med. Eng. Phys., vol. 29, no. 7, pp. 749754, 2007.
[11] H. Lin, J. Chen, and C. Chen, "A novel technology: microfluidic devices for microbubble ultrasound contrast agent generation, Med. Biol. Eng. Comput., vol. 54, no. 9, pp. 114, 2016.
[12] K. Hettiarachchi, E. Talu, M. L. Longo, P. a Dayton, and A. P. Lee, "On-chip generation of microbubbles as a practical technology for manufacturing contrast agents for ultrasonic imaging., Lab Chip, vol. 7, no. 4, pp. 463468, 2007.
[13] M. Seo, I. Gorelikov, R. Williams, and N. Matsuura, "Microfluidic assembly of monodisperse, nanoparticle-incorporated perfluorocarbon microbubbles for medical imaging and therapy, Langmuir, vol. 26, no. 17, pp. 1385513860, 2010.
[14] J. M. Zhang, E. Q. Li, and S. T. Thoroddsen, "A co-flow-focusing monodisperse microbubble generator, J. Micromechanics Microengineering, vol. 24, no. 3, p. 35008, 2014.
[15] S. Mance, L. Pages, A. Gu, P. Joseph, and F.- Toulouse, "Production of 3-10 μm microbubbles suited for ultrasonic imaging by 2.5D nanofluidic device, pp. 25622563, 2014.
[16] "Lantheus Medical Imagin g. Definity (perflutren lipid microsphere) injectable suspension. [Online]. Available: http://www.definityimaging.com/main.html.
[17] Y. Xia and G. M. Whitesides, "Soft lithography, Annu. Rev. Mat. Sci., vol. 28, no. 1, pp. 153184, 1998.
[18] B.-U. Moon, D. K. Hwang, and S. S. H. Tsai, "Shrinking, growing, and bursting: microfluidic equilibrium control of water-in-water droplets, Lab Chip, vol. 8, no. 14, pp. 198220, 2016.
[19] D. J. Cox and J. L. Thomas, "Rapid Shrinkage of Lipid-Coated Bubbles in Pulsed Ultrasound, Ultrasound Med. Biol., vol. 39, no. 3, pp. 466474, 2013.
[20] T. C. Merkel, V. I. Bondar, K. Nagai, B. D. Freeman, and I. Pinnau, "Gas sorption, diffusion, and permeation in poly(dimethylsiloxane), J. Polym. Sci. Part B Polym. Phys., vol. 38, no. 3, pp. 415434, 2000.
[21] T. Cubaud, M. Sauzade, and R. Sun, "CO2 dissolution in water using long serpentine microchannels, Biomicrofluidics, vol. 6, no. 2, pp. 19, 2012.
[22] S. Shim, J. Wan, S. Hilgenfeldt, P. D. Panchal, and H. a Stone, "Dissolution without disappearing: multicomponent gas exchange for CO2 bubbles in a microfluidic channel., Lab Chip, vol. 14, no. 14, pp. 242836, 2014.

978-1-5386-3383-0/17/$31.00 ©2017 IEEE